

phys. stat. sol. (b) **95**, 359 (1979)

Subject classification: 13.4 and 14.3; 22.4.4

*Institute of Physics, Polish Academy of Sciences, Warsaw*

## Energy Levels at $\Gamma$ -Point in $\text{Hg}_{1-x}\text{Mn}_x\text{Te}$ in Intense Magnetic Fields

By

P. BYSZEWSKI, K. SZLENK, J. KOSSUT, and R. R. GAŁĄZKA

Measurements of Shubnikov-de Haas effect in  $\text{Hg}_{1-x}\text{Mn}_x\text{Te}$  for  $x = 0, 0.02, 0.04, 0.09$  in magnetic fields up to 30 T are reported. The experiments are interpreted within a model which takes into account the exchange interaction of mobile electrons and 3d localized electrons of Mn. At very low temperatures the freeze-out effect is also observed.

Es wird der Shubnikov-de Haas-Effekt in  $\text{Hg}_{1-x}\text{Mn}_x\text{Te}$  für  $x = 0, 0.02, 0.04$  und  $0.09$  in Magnetfeldern bis zu 30 T gemessen. Die Ergebnisse werden mit einem Modell interpretiert, das die Austauschwechselwirkung von beweglichen Elektronen und lokalisierten 3d-Elektronen von Mn berücksichtigt. Bei sehr tiefen Temperaturen wird auch der Ausfriereffekt beobachtet.

### 1. Introduction

Mercury telluride containing a small amount of manganese is a diluted paramagnetic system. If the manganese concentration is low enough the exchange interaction between neighbouring Mn ions is negligible. The measurements of magnetic susceptibility [11] show that if the concentration increases the interaction between pairs has to be accounted for.

The band structure of  $\text{Hg}_{1-x}\text{Mn}_x\text{Te}$  mixed crystals at high magnetic fields is strongly modified as compared to the band structure of usual small-gap semiconductors like  $\text{HgTe}$ . This modification was shown [1 to 4] to be due to the exchange interaction between mobile conduction or valence electrons and 3d electrons localized at Mn ions. These modifications of the band structure manifest themselves as numerous anomalies in magnetotransport [1, 2] and magneto-optical [3, 4] properties of  $\text{Hg}_{1-x}\text{Mn}_x\text{Te}$ . In this paper we present a study of galvanomagnetic effects, namely the Shubnikov-de Haas effect and the freeze-out effect of  $\text{Hg}_{1-x}\text{Mn}_x\text{Te}$  at very strong magnetic fields up to 30 T. The determination of band structure parameters is more reliable when the electron concentration in the studied samples covers a wide range. Therefore, we used samples with  $10^{17}$  to  $10^{18} \text{ cm}^{-3}$  electrons for Shubnikov-de Haas effect measurements and samples with  $10^{15} \text{ cm}^{-3}$  electrons for freeze-out experiments. Although it is in principle possible to observe the Shubnikov-de Haas oscillations at fields in the range 2 to 10 T, the observation of the SdH peaks related to Landau levels characterized by small values of quantum number  $n$  is possible only in stronger fields (15 to 30 T). The position of these peaks is very sensitive to the exchange coupling constants. It is therefore important to include the observed positions of these peaks into the numerical fitting procedure in order to increase its credibility. The freeze-out experiments require the usage of very strong magnetic fields, too: only then it is possible to see the influence of extrinsic carriers, because in the case of zero-gap materials the intrinsic carriers often mask the contribution of the extrinsic carriers. Nevertheless in very strong magnetic fields we succeeded in observing the freeze-out effect and we were able to determine a ionization energy of impurities. The impurity level proved to be in the energy gap induced by the magnetic field.

## 2. Experimental Technique and Results

Monocrystalline samples of  $\text{Hg}_{1-x}\text{Mn}_x\text{Te}$  ( $x = 0, 0.02, 0.04, 0.09$ ) were studied. Their parameters are listed in Table 1. The measurements were performed in a pulsed magnetic field using a continuous flow cryostat. The apparatus was described in [5]. The temperature was controlled by means of a helium flow and a heater and was measured by a thermocouple. In order to reduce the heating of the high-resistivity samples the current applied to the samples had the form of a rectangular wave with stabilized height. The magnetoresistivity and Hall voltage were recorded using a digital memory.

The Shubnikov-de Haas oscillations (Fig. 1) were observed in the case of samples with high electron concentration. The SdH peak positions were temperature-dependent. Some of the peaks exhibited a splitting when the temperature was increased. We observed a difference between the positions of SdH peaks in longitudinal and transverse configuration: the peaks in the longitudinal case were shifted toward higher magnetic fields. We were also able to observe the freeze-out of the carriers in the case of samples with low electron concentration, although the materials in question are zero-gap semiconductors. The Fermi level in these samples was also degenerate with the conduction band and lay 1.3 meV above  $\Gamma_8$ -energy at zero field. The resistivity of these samples is very small at low magnetic fields and it rapidly increases when the magnetic field rises. Also the Hall voltage changes its sign from negative to positive when the field is increased. This fact indicates that at  $H = 0$  a small number of mobile electrons determines the conductivity. When the magnetic field is applied the contribution of holes becomes apparent. In the case of  $\text{Hg}_{1-x}\text{Mn}_x\text{Te}$  with zero gap at  $H = 0$  a negative magnetoresistance was observed in the range 2 to 10 T. Above 10 T when the energy gap induced by the field starts to open we observe the freeze-out effect of intrinsic and extrinsic carriers.

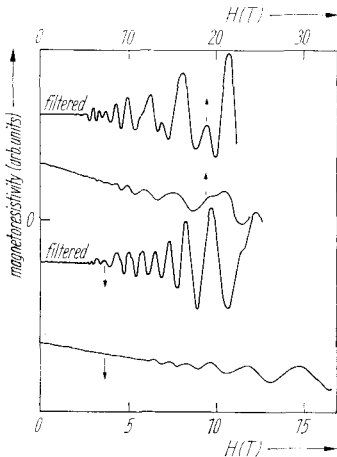


Fig. 1

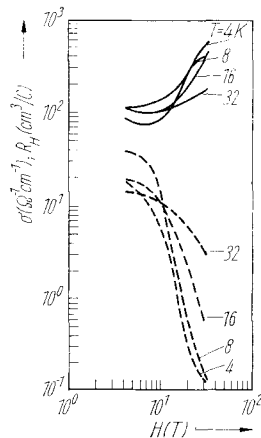


Fig. 2

Fig. 1. Typical Shubnikov-de Haas oscillation recordings for  $\text{Hg}_{0.98}\text{Mn}_{0.02}\text{Te}$ . The voltages were measured at two different horizontal scales. Only six peaks at high field are shown in Fig. 5. In order to obtain better resolution at the SdH oscillations we recorded also voltages filtered by 100 to 400 Hz band filters (upper curves). It helps only to find double peaks, yet introduces a phase shift.  $n = 2.4 \times 10^{18} \text{ cm}^{-3}$ ,  $T = 4 \text{ K}$ .

Fig. 2. Hall constant  $R_H$  (—) and conductivity  $\sigma$  (---) of the sample  $D_3$  of  $\text{Hg}_{0.98}\text{Mn}_{0.02}\text{Te}$  at different temperatures

Table 1

sample	$x$	$N_D$ ( $10^{17} \text{ cm}^{-3}$ )	$N_A$ ( $10^{16} \text{ cm}^{-3}$ )
—	0.02	24	—
—	0.02	4.6	—
—	0.02	7.5	—
—	0.04	7.2	—
—	0.04	10	—
—	0.04	14	—
—	0.09	9.4	—
—	0.09	6.5	—
—	0.09	5.8	—
—	0.09	2.9	—
—	0.09	2.1	—
A <sub>11</sub>	0	—	0.2
A <sub>12</sub>	0	—	1
A <sub>2</sub>	0	—	8
D <sub>1</sub>	0.02	—	12
D <sub>2</sub>	0.02	—	8
D <sub>3</sub>	0.02	—	5.5
E	0.03	—	2.7
F	0.04	—	14

Fig. 2 presents the magnetic field induced changes of  $R_H$  and  $\sigma$ .  $R_H(H)$  reflects the free-hole concentration and the magnetoconductivity  $\sigma$  the mobility and concentration changes. Unfortunately, the available magnetic fields were not strong enough to enable the determination of the position of the acceptor levels in all samples. Nevertheless we were able to do so in the case of some samples. The interpretation of the experimental data was based on the analysis of the conductivity tensor components, which are related to the resistivities measured in experiments,

$$\sigma_{xx} = \frac{\varrho_{xx}}{\varrho_{xx}^2 + \varrho_{xy}^2}, \quad \sigma_{xy} = \frac{\varrho_{xy}}{\varrho_{xx}^2 + \varrho_{xy}^2}.$$

The typical behaviour of  $\sigma_{xx}$  and  $\sigma_{xy}$  is shown in Fig. 3. The classical considerations for the conductivity in a strong magnetic field give  $\sigma_{xx} < \sigma_{xy}$ . In the region of magnetic field where the classical treatment is not applicable we restricted ourselves to the consideration of the  $\sigma_{xy}$ -component only, since the expressions for it are identical in both classical and quantum approaches.

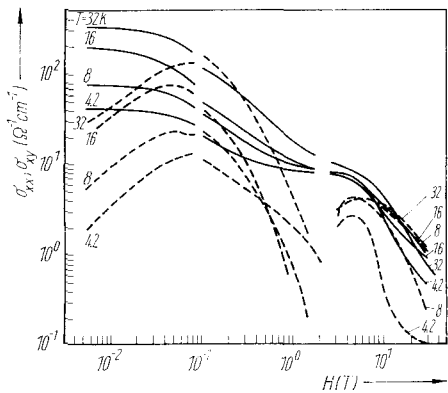


Fig. 3. The conductivity tensor components  $\sigma_{xx}$  (—) and  $\sigma_{xy}$  (---) for sample A<sub>2</sub> of HgTe. Low-field measurements were performed in steady fields

### 3. Interpretation

$\text{Hg}_{1-x}\text{Mn}_x\text{Te}$  mixed crystals exhibit either an inverted band structure (for  $x < 0.07$  at 4.2 K) or a simple InSb-like band structure (for  $x > 0.07$  at 4.2 K). Therefore, we were able to study both kinds of structure.

In the presence of a magnetic field the band structure is strongly influenced by the exchange interaction of mobile electrons and 3d electrons of manganese. Our interpretation is based on a theoretical model which takes this interaction into account apart from the usual Hamiltonian describing a narrow-gap semiconductor in a quantizing magnetic field [8]. The model was described in detail in [2, 3] and therefore we outline only its main features here. The usual Pidgeon and Brown matrices [8] are supplemented by elements having their origin in the exchange interaction which is assumed in a simple Heisenberg form,

$$H_{\text{int}} = \sum_i J(\mathbf{r} - \mathbf{R}_i) \boldsymbol{\sigma} \cdot \mathbf{S}_i,$$

where  $\boldsymbol{\sigma}$  is the conduction electron spin,  $\mathbf{S}_i$  the total spin of the  $i$ -th manganese ion, and  $J$  the exchange integral. When an average value of the manganese spin is taken over all existing Mn ions the additional matrix elements are the following:

$$D_{a'} = \begin{pmatrix} \frac{N\alpha\langle S_z \rangle}{2} & 0 & 0 & 0 \\ 0 & \frac{N\beta\langle S_z \rangle}{2} & 0 & 0 \\ 0 & 0 & -\frac{N\beta\langle S_z \rangle}{6} & \frac{-i\sqrt{2} N\beta\langle S_z \rangle}{3} \\ 0 & 0 & \frac{i\sqrt{2} N\beta\langle S_z \rangle}{3} & \frac{N\beta\langle S_z \rangle}{6} \end{pmatrix},$$

$$D_{b'} = \begin{pmatrix} -\frac{N\alpha\langle S_z \rangle}{2} & 0 & 0 & 0 \\ 0 & \frac{N\beta\langle S_z \rangle}{6} & 0 & \frac{i\sqrt{2} N\beta\langle S_z \rangle}{3} \\ 0 & 0 & -\frac{N\beta\langle S_z \rangle}{2} & 0 \\ 0 & \frac{-i\sqrt{2} N\beta\langle S_z \rangle}{3} & 0 & \frac{-N\beta\langle S_z \rangle}{6} \end{pmatrix},$$

where  $\alpha = \langle S | J | S \rangle$ ,  $\beta = \langle X | J | X \rangle$ , and  $S$ ,  $X$  are s-like and p<sub>x</sub>-like Kohn-Luttinger amplitudes of the conduction electron wave functions,  $\langle S_z \rangle$  is the average value of  $z$ -component of Mn spin,  $N$  the number of Mn ions per unit volume.  $\langle S_z \rangle$  is proportional to the magnetization of the samples, so it could be taken from an independent experiment. Unfortunately, only in the case of  $x = 0.02$  such measurements were available.<sup>1)</sup> In the case of  $x = 0.04$  and  $0.09$  values of  $\langle S_z \rangle$  were treated as an additional fitting parameter. Namely,  $\langle S_z \rangle$  was calculated in a simple model including non-interacting isolated Mn ions and pairs of exchange coupled Mn ions (see [2]). Assuming that the distribution of Mn ions is random there is only one parameter in

<sup>1)</sup> In [2] there is an error. Fig. 3 shows the magnetization for  $x = 0.02$  and not for  $x = 0.01$  as written there.

Table 2  
 Band structure parameters

$x$	0.00	0.02	0.04	0.09
$E_0(4.2 \text{ K}) \text{ (eV)}$	-0.303	-0.185	-0.1	0.045
$P \text{ (} 10^{-8} \text{ eV cm)}$	8.3	8.2	8.0	8.0
$A \text{ (eV)}$	1.08	1.08	1.08	1.08
$\gamma_1$	3.0	3.0	3.0	3.0
$\gamma_2$	-0.5	-0.5	-0.5	-0.5
$\gamma_3$	0.67	0.67	0.67	0.67
$\kappa$	-1.3	-1.3	-1.3	-1.3
$F$	0	0	0	0
$\alpha \text{ (eV)}$	0	-0.65	-0.6	-1.4
$\beta \text{ (eV)}$	0	1.4	1.3	2.3
$I \text{ (K)}$	0	3.0	24.0	14.0

this model, namely the exchange constant within a manganese pair. Exactly the same model was used in the case of  $x = 0.04$  and  $0.09$  samples, although one may question its applicability in the case of  $x = 0.09$ . We fitted the position of the observed SdH peaks to the theoretically calculated field of coincidence of the Fermi level with the bottoms of the Landau levels. For the computations we used the parameters listed in Table 2. The band structure in magnetic field depends on all parameters listed in Table 2. However, the Shubnikov-de Haas oscillation position is in the first place influenced by the exchange interaction parameters  $\alpha$ ,  $\beta$ , and the Mn-Mn exchange constant. The other parameters change both the density of states and the position of the crossing points of Fermi energy with Landau levels. We used for our computation the complete set of other parameters (Table 2) determined from other experiments on HgTe and HgMnTe. In this way we obtained  $\alpha$  and  $\beta$  (and the exchange Mn-Mn constant in the case of  $x = 0.04$  and  $0.09$ ). For  $x = 0.02$  and  $0.04$  we obtained  $\alpha$  and  $\beta$  which were compatible with the earlier estimations [2, 3]  $\alpha = -0.65$ ,  $\beta = 1.4$  eV for  $x = 0.02$  and  $\alpha = -0.6$ ,  $\beta = -1.3$  eV for  $x = 0.04$ . The fitted value of the Mn-Mn exchange constant for  $x = 0.04$  corresponds to the magnetization shown in Fig. 8. The comparison of the theory and experimental SdH peak positions is presented in Fig. 5 to 7. To visualize the influence of the exchange interaction  $H_{\text{int}}$  the energy structure of HgTe in magnetic field is shown in Fig. 4. For  $x = 0.09$  the fitted values of  $\alpha$  and  $\beta$  are considerably higher than for  $x = 0.02$  and  $0.04$ , namely  $\alpha = -1.4$  and  $\beta = 2.3$  eV. It must be said, however, that the numerical fit is not very good. Moreover, the simple description of magnetization might be wrong in the case of  $x = 0.09$ .

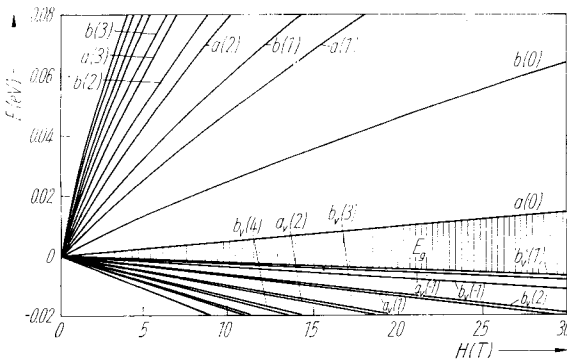


Fig. 4. The Landau levels of HgTe in magnetic field at 4 K

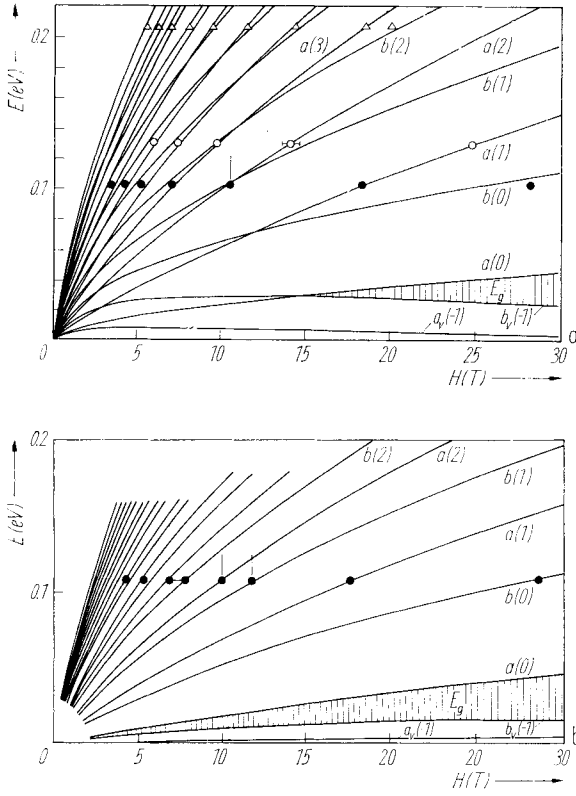


Fig. 5. The energy levels of  $\text{Hg}_{0.98}\text{Mn}_{0.02}\text{Te}$  in magnetic field (measured from the  $\Gamma_8$  energy band at zero magnetic field). The dots represent the position of the observed peaks in Shubnikov de Haas experiments. a) at 4 K,  $n = \bullet 4.6 \times 10^{17}$ ,  $\circ 7.5 \times 10^{17}$ ,  $\Delta 2.4 \times 10^{18} \text{ cm}^{-3}$ ; b) at 36 K,  $n = 4.6 \times 10^{17} \text{ cm}^{-3}$ . Marks indicate the peak which splits at higher temperatures

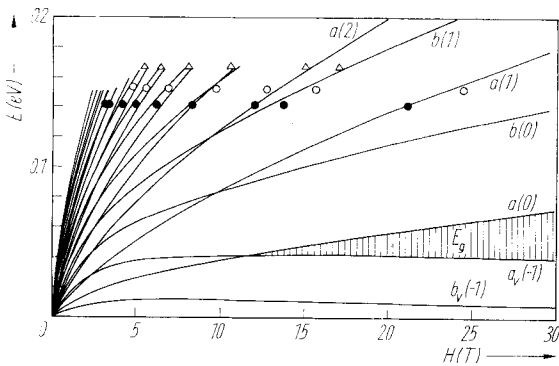


Fig. 6. Energy levels of  $\text{Hg}_{0.96}\text{Mn}_{0.04}\text{Te}$ . Dots represent positions of SdH maxima at 4 K (measured from the  $\Gamma_8$  energy band at zero magnetic field).  $n = \bullet 7.2 \times 10^{17}$ ,  $\circ 1 \times 10^{18}$ ,  $\Delta 1.4 \times 10^{18} \text{ cm}^{-3}$

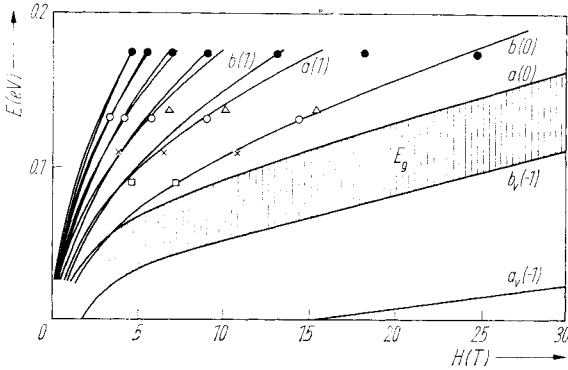


Fig. 7. Energy levels of  $\text{Hg}_{0.91}\text{Mn}_{0.09}\text{Te}$  measured from the  $\Gamma_6$  band energy at zero field at 4 K.  $\bullet$   $n = 9.4 \times 10^{17}$ ,  $\triangle$   $6.5 \times 10^{17}$ ,  $\circ$   $5.8 \times 10^{17}$ ,  $\times$   $2.9 \times 10^{17}$ ,  $\square$   $2.1 \times 10^{17} \text{ cm}^{-3}$

A striking feature of the band structure of  $\text{HgMnTe}$  in magnetic field is that contrary to usual zero-gap semiconductors [6, 7] the magnetic field does not open the gap in the low-field region. A considerable strength of the field is required in order to do so and above this value of the field the band structure starts to resemble the usual situation, e.g. of  $\text{HgTe}$ . It might be seen in Fig. 5, 6 that the levels belonging to different sets (corresponding to different values of  $j_z$ , the total angular momentum) intersect each other. It may then happen that the Fermi energy coincides with a pair of intersecting levels leading to only one peak in SdH experiment. But the field at which the intersection occurs depends sensitively on temperature (through the  $\langle S_z \rangle$  temperature dependence). So when the temperature is increased the Fermi level coincides with two well-separated levels (which intersected at lower temperature) producing two peaks in resistivity. This fact explains the splitting of some peaks appearing at higher temperatures, indicated by the marks in Fig. 5 a and b.

The SdH measurements allowed to determine the conduction band structure and to check the theoretical model described in [3, 4], only the energy gap dependence on magnetic field deduced from this model remains uncertain. Our experiments performed on pure  $\text{Hg}_{1-x}\text{Mn}_x\text{Te}$  samples showed that at intermediate fields where negative magnetoresistivity was observed, the valence and conduction bands overlap. At high field, in the region of the freeze-out effect, the magnetic field induces an energy gap. The experiments on the freeze-out effect prove that the magnetic field opens the energy gap even in manganese-mercury telluride compounds. These experiments supply also information on the position of acceptor levels [9, 10]. Because the freeze-out effect was observed at very high fields and low temperatures, therefore,

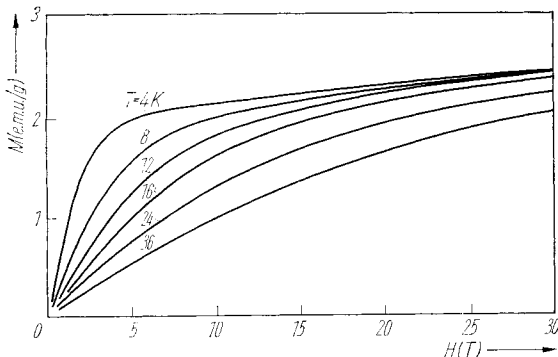


Fig. 8. The magnetization of  $\text{Hg}_{0.96}\text{Mn}_{0.04}\text{Te}$  fitted to the SdH peak positions at various temperatures

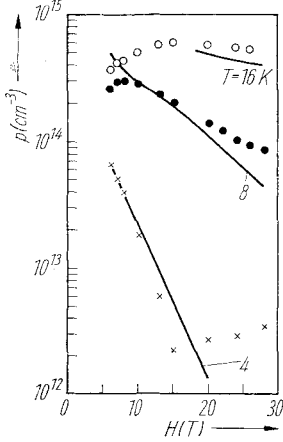


Fig. 9

Fig. 9. Hole concentration in sample A<sub>11</sub> of HgTe. Dots experimental values, full lines computed values

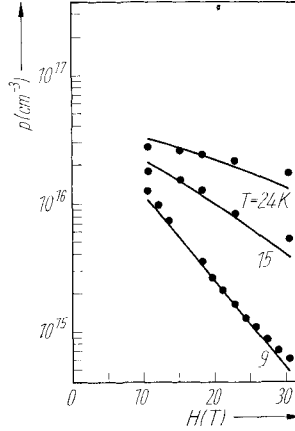


Fig. 10

Fig. 10. Hole concentration in sample D<sub>2</sub> of Hg<sub>0.98</sub>Mn<sub>0.02</sub>Te. Dots experimental values, full lines computed values

to interpret these data we performed computations based on a model assuming a single acceptor energy which depends linearly on magnetic field.

The free-hole concentrations determined from experiments are shown in Fig. 9 and 10. These results are compared with the theoretical concentration of holes found by solving the neutrality equation

$$n + \frac{N_A}{1 + 4 \exp\left(\frac{E_0 + bH}{k_0 T} - \eta\right)} = p$$

with  $n(p)$  free-electron (hole) concentration,  $N_A(N_D)$  acceptor (donor) concentration. This equation was solved for two models: (i) of a quantized valence band [10] and (ii) of a classical valence band. In the first model both the band energy and acceptor energy depend on magnetic field and the ionization energy is a sum of the two values. In the second model only the acceptor energy is a function of magnetic field. In both

cases the total acceptor ionization energy to the valence band was assumed to change linearly with magnetic field ( $E_A = E_0 + bH$ ). The parameters  $E_0$ ,  $b$ , and  $N_A$  were varied to find the best fit of computed and measured concentrations. It was found that quantization has a negligible effect on ionization energy and  $N_A$ , determined in both cases by fitting the theoretical values to the measured ones. The set of best

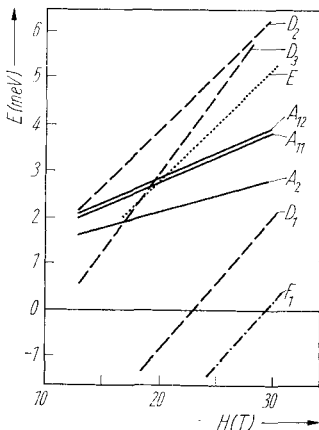


Fig. 11. Acceptor ionization energy determined from the freeze-out experiment in Hg<sub>1-x</sub>Mn<sub>x</sub>Te.  $x =$  ——— 0, ——— 0.02, ..... 0.03, - - - - 0.04



parameters is shown in Fig. 11 and Table 1. The total ionization energy is a parameter directly determined in experiment and we show it in Fig. 11 to better describe the measured values than the acceptor energy (the values coincide only in case of the second model). The ionization energies determined at high magnetic field differ substantially from those found by magneto-optical measurements at low fields. We suppose that the freeze-out effect is sensitive to the lowest energy level, whereas the magneto-optical experiments to the density-of-states peaks associated with all Landau levels. The freeze-out experiments show in some cases a saturation of concentration at very high field and low temperature (Fig. 9). The assumed theoretical model of a single acceptor level cannot explain such results. Perhaps, the reason for this disagreement is the assumption about the linear dependence of the acceptor level on magnetic field.

#### 4. Conclusions

The theoretical model of the exchange interaction of localized magnetic moments with valence and conduction electrons describes well the energy structure in intense magnetic fields. The exchange interaction strongly affects the structure, but the application of the external magnetic field of high intensity restores the usual energy level configuration and opens the energy gap. It is possible to observe the freeze-out effect even in these zero-gap materials. The samples required for this purpose should possess the Fermi level (at zero field) inside the conduction band close to the top of the valence band. These measurements supply information on impurity level energy. However, the single impurity level model used in the interpretation is too crude and cannot explain all the experimental data.

#### Acknowledgements

Our gratitude is due to Dr. W. Dobrowolski for his great help in numerical calculations and Mgr. A. Mongird-Gorska for her help in some of the experiments.

#### References

- [1] M. JACZYŃSKI, J. KOSSUT, and R. R. GAŁĄZKA, Proc. III. Internat. Conf. Phys. Narrow-Gap Semicond., PWN, Warsaw 1978 (p. 325).
- [2] M. JACZYŃSKI, J. KOSSUT, and R. R. GAŁĄZKA, phys. stat. sol. (b) **88**, 73 (1978).
- [3] G. BASTARD, C. RIGAU, and A. MYCIELSKI, phys. stat. sol. (b) **79**, 585 (1977).
- [4] G. BASTARD, C. RIGAU, Y. GULDNER, J. MYCIELSKI, and A. MYCIELSKI, J. Physique **39**, 87 (1978).
- [5] P. BYSZEWSKI, M. CIEPLAK, and K. SZYMBORSKI, Cryogenics **18**, 56 (1978).
- [6] J. KOWALSKI and W. ZAWADZKI, Solid State Commun. **13**, 1433 (1973).
- [7] P. BYSZEWSKI, E. Z. DZIUBA, R. R. GAŁĄZKA, K. SZLENK, K. SZYMBORSKI, and W. WALUKIEWICZ, phys. stat. sol. (b) **71**, 117 (1975).
- [8] C. R. PIDGEON and R. BROWN, Phys. Rev. **146**, 575 (1966).
- [9] P. BYSZEWSKI and R. R. GAŁĄZKA, phys. stat. sol. (b) **84**, K83 (1977).
- [10] P. BYSZEWSKI, K. SZLENK, and R. R. GAŁĄZKA, see [1] (p. 191).
- [11] U. SONDERMANN, private communication.

(Received May 2, 1979)